Eur Biophys J (2012) 41:597–605
DOI 10.1007/s00249-012-0827-3

ORIGINAL PAPER

EBSA
Biophysics in Europe

HuR thermal stability is dependent on domain binding and upon phosphorylation

Rafael Manfred Scheiba · Ángeles Aroca · Irene Díaz-Moreno

Received: 13 December 2011 / Revised: 10 May 2012 / Accepted: 28 May 2012 / Published online: 17 June 2012

Abstract Human antigen R (HuR) is a multitasking RNA binding protein involved in posttranscriptional regulation by recognizing adenine- and uracile-rich elements placed at the 3′-untranslated regions of messenger RNAs (mRNAs). The modular architecture of the protein, which consists of two N-terminal RNA recognition motifs (RRMs) in tandem spaced from a third one by a nuclear-cytoplasmic shuttling sequence, controls the stability of many mRNA targets, as well as their translation rates. A higher level of regulation comes from the fact that both localization and function of HuR are strictly regulated by phosphorylation. Here, we report how the thermal stability of RRM2 is decreased by the presence of RRM1, indicating that both domains are interacting in solution. In addition, even though no significant structural changes are observed among mutants of HuR RRM12 mimicking phosphorylated species, slight differences in stability are appreciable, which may explain the RNA binding activity of HuR.

Keywords HuR · Phosphorylation · Posttranslational modifications · RNA binding protein · RNA recognition motif · Protein thermal stability

Abbreviations

AREs	Adenine- and uracile-rich elements
CARM1	Coactivator-associated arginine methyltransferase 1 protein
CD	Circular dichroism
Chk2	Checkpoint 2 kinase
Cdk	Cyclin-dependent kinase 1
DSF	Differential scanning fluorimetry
DTT	Dithiothreitol
ELAV	Embryonic lethal and abnormal vision
HNS	Human novel shuttling
HuR	Human antigen R
HuR FL	HuR full-length
K_D	Dissociation affinity constant
PKCα	Protein kinase C α
PKCδ	Protein kinase C δ
RBP	RNA binding protein
RMSD	Root-mean-square deviation
RRM	RNA recognition motif
RRM12 WT	RRM12 *wild-type*
RT-PCR	Real-time polymerase chain reaction
T_m	Midpoint melting temperature
UTRs	Untranslated regions

R. M. Scheiba · Á. Aroca · I. Díaz-Moreno (✉)
Instituto de Bioquímica Vegetal y Fotosíntesis, cicCartuja, Universidad de Sevilla-CSIC, Americo Vespucio 49, 41092 Sevilla, Spain
e-mail: idiazmoreno@us.es

Introduction

Human antigen R (HuR) is a ubiquitous 36-kDa RNA binding protein (RBP) consisting of three RNA recognition motifs (RRMs; Birney et al. 1993; Ma et al. 1996). HuR (also known as ELAV-like protein 1) plays a key role in the cell cycle, stress stimuli, inflammation, and cancer. HuR controls such functions by recognizing the adenine- and uracile-rich elements (AREs) placed at the 3′-untranslated regions (UTRs) of certain RNAs (Abdelmohsen et al. 2007a; Brennan and Steitz 2001; Dixon et al. 2001; Gorospe 2003; Sengupta et al. 2003). As a consequence, the expression level of these RNA targets is affected, so dependent processes in the cell are regulated. In fact, HuR has been characterized as

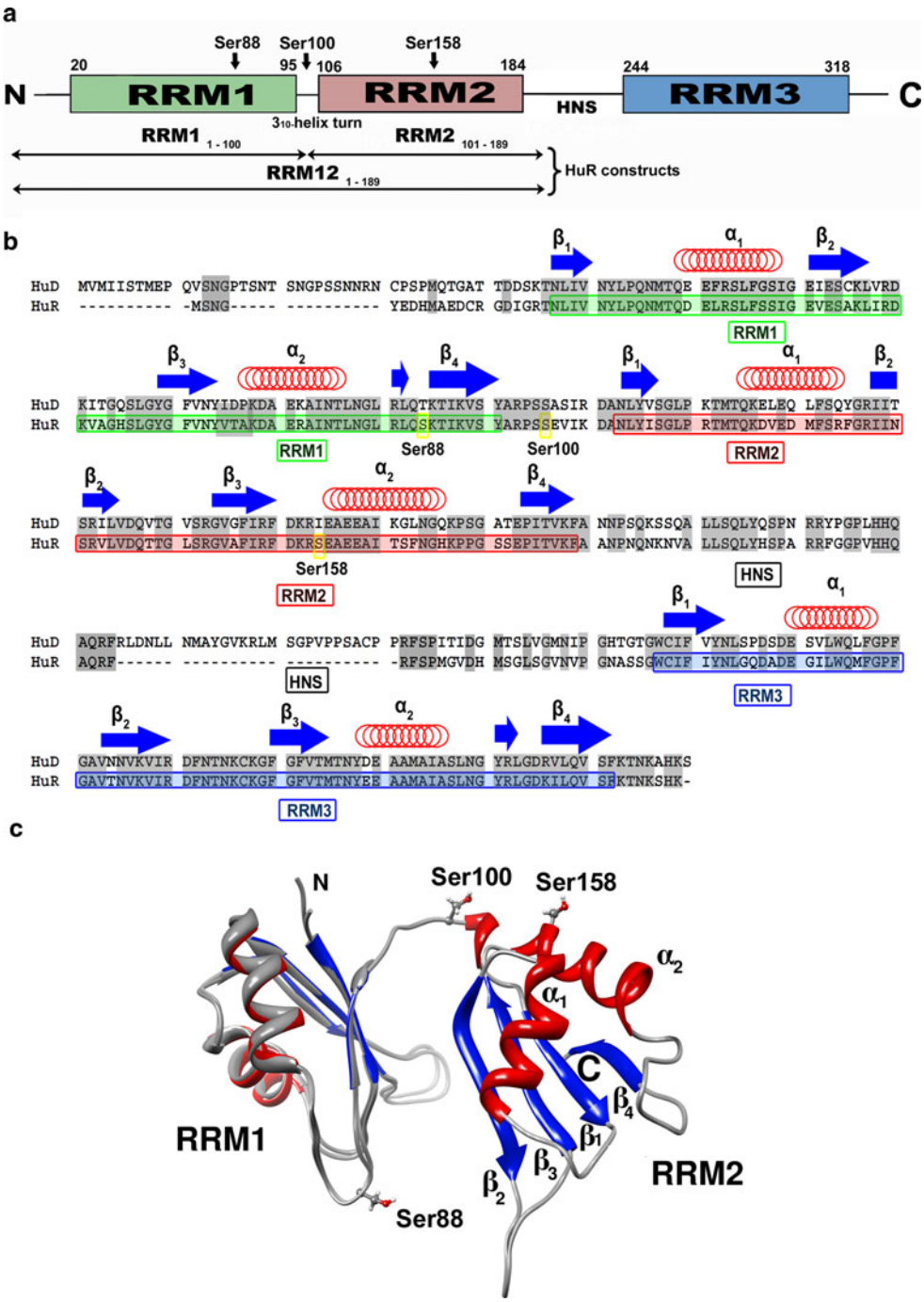

Fig. 1 HuR protein. **a** Schematic domain organization of HuR and constructs used in this study. **b** Sequence alignment of HuR and its homologous HuD protein. *Green*, *red*, and *blue boxes* highlight RRM1, RRM2, and RRM3 domains, respectively. HNS is also represented. Secondary structure elements are marked by *blue arrows* for β-strands and *red coil symbols* for α-helices based on the prediction using PSIPRED server. Phosphorylation sites of serines, which have been mutated in this study, are framed in *yellow boxes*. **c** Superposition between the crystal structure of HuR RRM1 (PDB entry 3HI9; Benoit et al. 2010) and the homology model of HuR RRM12 built as described in "Materials and methods." The RMSD for backbone atoms of HuR RRM1 domain in both structures is 0.583 Å. Side-chains of serine residues to be phosphorylated are included

an antiapoptotic switch tightly regulated by posttranscriptional orchestration (Abdelmohsen et al. 2007a). However, it has been recently reported that proapoptotic reactions can also be supported, which depend on the caspase-mediated cleavage of HuR (Mazroui et al. 2008).

It is worth mentioning that there are many studies concerning the behavior of HuR in the cellular environment, although little is known about the structure and the related molecular mechanisms of this RBP. HuR is a multidomain protein whose three RRMs show the canonical topology: $\beta_1\alpha_1\beta_2\beta_3\alpha_2\beta_4$. Interestingly, the most N-terminal RRM domains—named RRM1 and RRM2—are in tandem, only separated by a 3_{10}-helix turn, whereas the C-terminal RRM3 motif is spaced by a 60-residue linker spanning the hinge called the human novel shuttling (HNS) sequence (Fig. 1a; Fan and Steitz 1998). Actually, HNS is known to determine the cellular localization of HuR either in the nucleus or the cytoplasm. Recently, the crystal structure of the first N-terminal RRM domain was solved (Benoit et al. 2010), although the global protein structure remains unknown.

Posttranslational modifications play an essential role in the cellular function of HuR. Recent research has revealed several phosphorylation sites in HuR which influence the interaction with its RNA targets and with other proteins and even its cellular localization (Abdelmohsen et al. 2007b; Doller et al. 2008; Kim and Gorospe 2008; Kim et al. 2008a, b). Such phosphorylations can be performed by different kinases such as checkpoint 2 kinase (Chk2), cyclin-dependent kinase 1 (Cdk1), and protein kinases C α or δ (PKCα or PKCδ). Upon HuR phosphorylation, different cellular responses have been described (Abdelmohsen et al. 2007a, b; Doller et al. 2008; Kim and Gorospe 2008; Kim et al. 2008a, b). Whereas the HuR capability for binding to RNA targets increases or decreases when Chk2 phosphorylates HuR at Ser88 or Ser100 residues, respectively (Abdelmohsen et al. 2007b), the addition of a phosphate group to Ser158, Ser221, and Ser318 by PKC favors the cytoplasmic localization of HuR instead of the preferred nuclear localization of the protein (Doller et al. 2008, 2009), along with an enhancement in the mRNA binding (Doller et al. 2007). In addition to Ser221 at HNS, HuR also becomes phosphorylated at Ser242, which is also involved in the nucleocytoplasmic shuttling (Kim et al. 2008b). The HuR shuttling can provide information about the cell state. Indeed, an increase of cytoplasmic HuR levels is an indicator for the stress response of the cell (Gorospe 2003) or different kinds of cancer (Denkert et al. 2004; Heinonen et al. 2005).

An additional HuR posttranslational modification consists of methylation at Arg117 by coactivator-associated arginine methyltransferase 1 (CARM1) protein (Li et al. 2002).

Given that both functionality and localization of HuR are strictly regulated by phosphorylation, exploring the stability of its N-terminal RRM domains after being posttranslationally modified would be highly valuable to understand the pleiotropic role of HuR in mRNA metabolism. Within this frame, this work suggests that the domains RRM1 and RRM2 as a cooperative assembly remains unchanged upon phosphorylation events of three Ser residues localized inside RRM motifs (the nonconserved Ser88 and Ser158 at RRM1 and RRM2, respectively) and at the interdomain linker (Ser100, highly conserved among the family members HuB, HuC, and HuD, as well as the ELAV—embryonic lethal and abnormal vision—*Drosophila* homolog).

Materials and methods

Site-directed mutagenesis of HuR RRM constructs

pGEX 5X2 vectors containing the sequences coding for HuR *full-length* (HuR FL) as well as individual N-terminal RRM domains—RRM1 and RRM2—and the two-domain construct RRM12, were kindly provided by Dr. M. Gorospe (National Institutes of Health, Baltimore, USA) and Dr. J. A. Steitz (Yale University, New Haven, USA). These genes were further cloned into the pGEX-4T2 vector, which was modified for RRM12 and HuR FL as follows: The GST sequence was substituted by a 6xHis-tag using the following primers: 5′ CATCATCACCACCATCACct ggttccgcgtggatccccagg 3′ (forward primer) and 5′ GTGAT GGTGGTGATGATGcatgaatactgtttcctgtgtg 3′ (reverse primer) to facilitate purification. Both GST and 6xHis tags were cleaved with thrombine, resulting in a short additional amino acid sequence for all constructs "GSPGIPSNYEDH," with a negligible effect on the secondary structure analysis. Serines at positions 88, 100, and 158 of the RRM12 construct were replaced by alanines or aspartates by site-directed mutagenesis (Mutagenex, Piscataway, USA).

Protein expression and purification of HuR constructs

Recombinant proteins were expressed in *Escherichia coli* BL21-T1® (SIGMA, St. Louis, USA) cells as follows. Competent cells were transformed with plasmid DNA and were grown at 30 °C for HuR FL and at 37 °C for RRM1, RRM2, and RRM12 constructs, both in Luria Bertani (LB) medium supplemented with ampicillin (50 μg/ml). Protein expression was induced by addition of 1 mM isopropyl-1-thio-β-D-galactopyranoside (IPTG) once the culture reached OD_{600} of 0.6–0.8. After 5 h expression in LB medium at 30 °C for HuR FL and at 37 °C for the other constructs, cells were harvested by centrifugation at 7,000 g and further resuspended in 50 mM Tris buffer (pH 8.0) for storage at −80 °C. The HuR FL protein was resuspended in the same buffer but supplemented with 800 mM NaCl.

GST fusion proteins were purified using a Glutathione Sepharose High Performance Matrix (GE Healthcare, Piscataway, USA), whereas His-tagged constructs were purified by nickel affinity chromatography (Ni Sepharose™ Fast Flow Matrix; GE Healthcare, Piscataway, USA). All constructs were expressed with thrombine-cleavable GST or His tags (GE Healthcare, Piscataway, USA). To separate HuR RRM single domains from the cleaved GST protein, gel filtration chromatography (Sephadex G-75 matrix; SIGMA, St. Louis, USA) was performed.

Samples were concentrated to 80 μM in 10 mM sodium phosphate (pH 7.3) with 0.5 mM DTT. HuR FL was supplemented with 800 mM NaCl and 0.1 % Sarkosyl detergent to increase its solubility during all purification steps. Protein concentration was determined using spectrophotometry with predicted extinction coefficients. All molecular weights of the HuR constructs used in this work were verified by matrix-assisted laser desorption/ionization time-of-flight (MALDI-TOF) spectroscopy.

Circular dichroism spectroscopy

All circular dichroism (CD) spectra were recorded in the far-ultraviolet (UV) range (190–250 nm) at 298 K on a Jasco J-815 spectropolarimeter, equipped with a Peltier temperature-control system, using a 1-mm quartz cuvette. Protein concentration was 12 μM in 10 mM sodium phosphate buffer (pH 7.3) supplemented with 0.5 mM DTT. For each sample, 20 scans were averaged for further secondary structure analysis using CDPRO software (Sreerama and Woody 2000), which includes the algorithms CONTIN, SELCON, and CDSSTR, as well as the CLSTR option to compare with a set of proteins with similar folds.

Thermal unfolding experiments were carried out in a range of temperatures from 298 to 371 K. For all these assays, the HuR species at 12 μM final concentration were dissolved in 10 mM sodium phosphate (pH 7.3) with 0.5 mM DTT. Temperature was increased at a rate of 1 K per min with an error within ±0.1 K. Spectra were recorded at the scan rate, band width, and sensitivity of 200 nm min^{-1}, 1.0 nm, and 0.2°, respectively. Protein unfolding was monitored by recording the CD signal at 195, 208, and 235 nm. The experimental data were fitted to a two-state native-denatured model (Privalov 1979).

RNA binding was monitored by adding increasing amounts of protein to 4 μM AU-11-mer (AU-UUUUAUUUU) RNA in 10 mM sodium phosphate pH 7.3, 0.5 mM DTT solution. A temperature of 298 K was chosen to optimize the signal change upon protein binding. Each CD spectrum was the average of 10 scans. The integral of this averaged signal between 260 and 275 nm was fitted against the protein concentration according to Santoro and Bolen (1988).

Differential scanning fluorimetry

Thermal unfolding of HuR constructs was monitored by differential scanning fluorimetry (DSF), in the presence of fluorescent SYPRO Orange dye (Invitrogen, Carlsbad, CA, USA), by using an IQ5 multicolor real-time PCR detection instrument (BioRad; Niesen et al. 2007). The commercial dye [5,000× concentrate in dimethyl sulfoxide (DMSO)] was at least tenfold diluted in 10 mM sodium phosphate buffer (pH 7.3), supplemented with 0.5 mM DTT, and the HuR samples (10–40 μg protein) were added at 25 μL final volume. The thermal unfolding process was monitored between 293 and 369 K, increasing the temperature at a rate of 1 K per min. The values for the midpoint melting temperature (T_m) were calculated from the first derivative in Origin 8.0 (Microcal Inc.), and a nonlinear curve-fitting function was used (Privalov 1979).

Results

HuR RRM domains adopt a canonical topology with negligible changes in their secondary structure upon phosphorylation

The crystallographic structure of HuR RRM1—recently published by Benoit et al. (2010)—shows that the canonical RRM folding adopts the $\beta\alpha\beta\beta\alpha\beta$ topology.

We have obtained a homology model of HuR RRM12 construct (Fig. 1b, c) using the crystallographic structure of its homolog HuD RRM12 as a template (PDB entry 1FXL; Wang and Tanaka Hall 2001). Sequence identity to the target was 75.4 %, and the model was built with the SWISS-MODEL server (Arnold et al. 2006; Kiefer et al. 2009) and graphically represented using Chimera software (Pettersen et al. 2004). Figure 1c shows the superposition of both HuR structures: the homology model of RRM12 and the crystallographic structure of RRM1.

Our homology model is in good agreement with the secondary structure contents for HuR constructs. Figure 2 shows the normalized far-UV CD spectra of isolated RRM1 and RRM2 domains, the tandem RRM12, and the HuR FL protein. Notably, all HuR species show similar global secondary structures with minor differences, as summarized in Table 1. Whereas all constructs share similar β-strand and turn contents, RRM2 differs from RRM1 and RRM12 in its higher α-helix content.

RRM12 mutants, in which Ser88, Ser100, and Ser158 have been substituted by aspartic acid residues to mimic phosphorylation events, exhibit secondary structure as that of RRM12 *wild-type* (RRM12 WT). In addition, Ser-by-Ala control mutations show similar CD spectra (Fig. 3; Table 1).

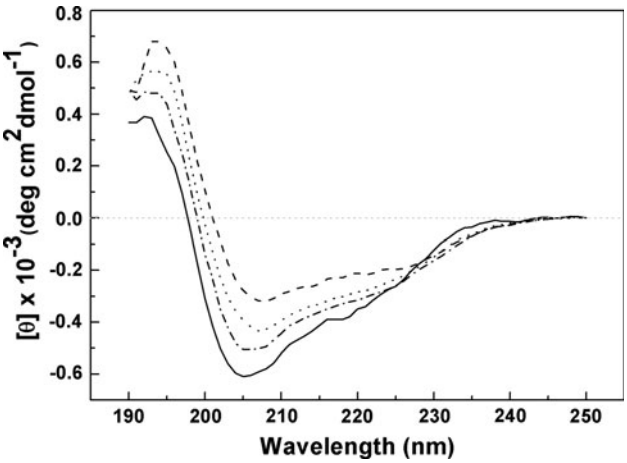

Fig. 2 Far-UV (190–250 nm) CD spectra of different HuR domain constructs. RRM domains are represented as follows: RRM1 by *solid line*, RRM2 by *dashed line*, RRM12 by *dotted line*, and HuR FL protein by *dash-dotted line*

Table 1 Percentage of secondary structure for the different constructs of HuR RRM domains and mutant species

Construct	α-Helix (%)	β-Strand (%)	Turn (%)	Unstructured (%)*
RRM1	6.01 ± 0.57	36.21 ± 1.25	19.49 ± 2.05	37.74 ± 3.95
RRM2	10.84 ± 0.22	34.11 ± 0.65	19.13 ± 0.90	30.81 ± 1.61
RRM12 WT	5.72 ± 0.77	39.67 ± 4.39	21.22 ± 1.80	33.03 ± 3.10
RRM12 S88D	11.03 ± 0.56	33.26 ± 2.05	19.64 ± 2.06	35.76 ± 4.75
RRM12 S88A	5.87 ± 0.44	39.00 ± 1.68	20.42 ± 1.41	34.25 ± 2.40
RRM12 S100D	5.34 ± 1.25	42.71 ± 4.30	19.25 ± 2.01	32.60 ± 3.81
RRM12 S100A	3.18 ± 0.39	40.88 ± 1.34	21.23 ± 1.15	34.78 ± 2.90
RRM12 S158D	5.14 ± 0.50	40.28 ± 1.58	20.51 ± 1.12	33.81 ± 3.17
RRM12 S158A	5.16 ± 0.34	39.79 ± 1.40	21.04 ± 1.65	33.75 ± 3.29
HuR FL	9.18 ± 1.79	34.95 ± 0.83	20.01 ± 2.39	35.23 ± 4.74

* This refers to both disordered and flexible and ordered but nonregular structured parts of the protein

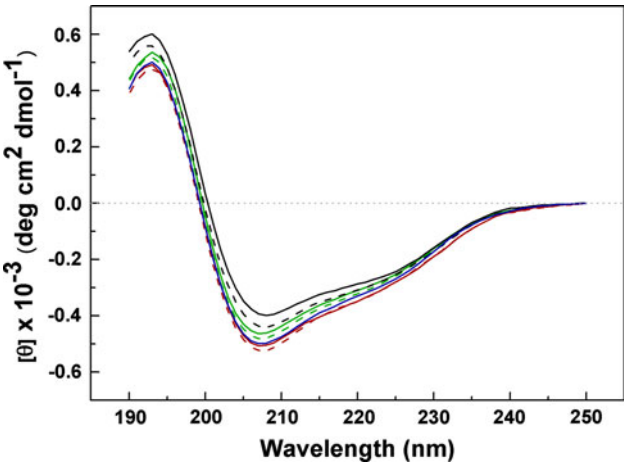

Fig. 3 Far-UV (190–250 nm) CD spectra of RRM12 WT and its phosphomimetic mutants. RRM12 WT is shown in *blue solid line*, RRM12-S88A in *green solid line*, RRM12-S88D in *green dashed line*, RRM12-S100A in *black solid line*, RRM12-S100D in *black dashed line*, RRM12-S158A in *red solid line*, and RRM12-S158D in *red dashed line*

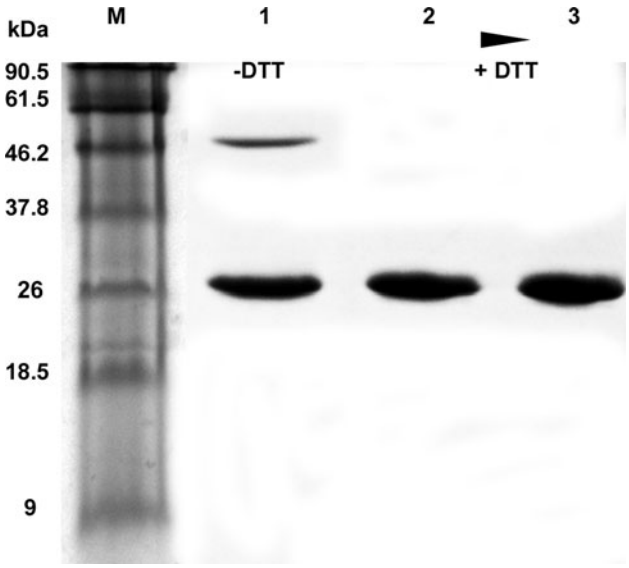

Fig. 4 SDS-PAGE electrophoresis of HuR RRM12 WT. *Line 1* HuR RRM12 WT sample devoid of DTT; *lines 2* and *3* protein samples previously incubated with 5 and 0.5 mM DTT, respectively, for 90 min before loading into the gel. In each line, 4 μg HuR RRM12 WT was loaded onto an 18 % SDS-PAGE gel. M: Pro-stain protein molecular weight marker (Intron Technologies Inc.)

For further investigation of the thermal stability of RRM12 WT and its mutants, the impact of Cys13 on the homodimer formation needs to be evaluated (Meisner et al. 2007; Benoit et al. 2010). Figure 4 shows a sodium dodecyl sulfate (SDS) polyacrylamide gel electrophoresis (PAGE) of RRM12 WT in absence and presence of dithiothreitol (DTT) at 0.5 and 5 mM, as reducing agent. RRM12 WT is clearly a monomer upon DTT addition, although the monomer–dimer equilibrium appears in samples devoid of DTT. These data were recently confirmed by analytical ultracentrifugation of RRM12 WT samples containing 0.5 mM DTT (data not shown). Thus, RRM12 WT construct, which includes Cys13, behaves as a monomer, at least in the experimental conditions used in this work.

Thermal stability of HuR RRM2 is decreased by the presence of RRM1

Recently, it has been demonstrated that the thermal stability of RNA binding domains reveals interactions between neighboring modules (Aroca et al. 2011; Díaz-Moreno et al. 2010). Thermal unfolding studies on the single N-terminal RRM segments and the two-domain construct from HuR were performed to confirm the assembly between RRM1 and RRM2, as inferred from the homology model of HuR RRM12 and the crystal structure of HuD RRM12 (Wang and Tanaka Hall 2001). CD spectroscopy shows that the T_m for isolated RRM1

Table 2 T_m values of HuR RRM domains and their phosphomimetic mutants, as calculated by CD and DSF

Constructs	T_m (K) by CD	T_m (K) by DSF
RRM1	335 ± 3	333 ± 1
RRM2	341 ± 2	339 ± 1
RRM12 WT	335 ± 2	332 ± 1
RRM12 S88D	336 ± 1	336 ± 2
RRM12 S88A	331 ± 1	330 ± 2
RRM12 S100D	334 ± 2	333 ± 1
RRM12 S100A	333 ± 1	330 ± 3
RRM12 S158D	330 ± 2	328 ± 3
RRM12 S158A	335 ± 1	330 ± 2

(335 ± 3 K) is lower than that for RRM2 (341 ± 2 K; Table 2). Interestingly, RRM12 is as stable as RRM1 (335 ± 2 K), suggesting that interdomain interactions are taking place. Such interaction lowers the T_m of RRM2 by ca. 6 K, as previously reported for other RNA binding proteins (Aroca et al. 2011; Díaz-Moreno et al. 2010). In addition, the denaturation curve of RRM12 is not the sum of the denaturation curves of the two individual RRM1 and RRM2 domains, revealing that only one transition state is observed (not two). Indeed, the cooperativity of the RRM12 denaturation is strongly reduced as compared with that of the individual domains.

These changes in stability between isolated RRM2 and RRM2 in RRM12 construct are confirmed by DSF, although ΔT_m is slightly higher (7 K; Table 2; Fig. 5a). Intriguingly, the T_m values calculated by DSF for HuR species are always equal to or lower than those estimated by CD, although ΔT_m is quite independent of the technique used (Table 2).

Stability of HuR RRM12 is regulated by phosphorylation

To analyze the phosphorylation effect of serine residues on the stability of HuR RRM12 construct, this posttranslational modification was mimicked by Ser-to-Asp substitutions. Even though use of Ser/Asp mutations simulates a constitutively phosphorylated protein with only one negative charge, it is herein extensively recommended since two out of three serine residues of RRM12 WT—those at positions 88 and 100—become phosphorylated by the same kinase, Chk2, making in vitro kinase assays undesirable.

The nonconserved serine residues, which are localized inside the RRM core, play an essential role in the stability of HuR RRM12. It is worth mentioning that phosphorylation at Ser88 in RRM1 mimicked by the S88D mutant makes the RRM12 construct slightly more stable than its control mutant (S88A) and RRM12 WT. Indeed, T_m of RRM12 S88D is increased by >5 K, using both CD and DSF approaches (Table 2; Fig. 5b). In contrast, the addition of a negatively charged group at position 158 (mutation S158D) slightly destabilizes HuR RRM12 with regard to the S158A mutant and RRM12 WT, despite the discrepancies in ΔT_m between CD and DSF. The well-

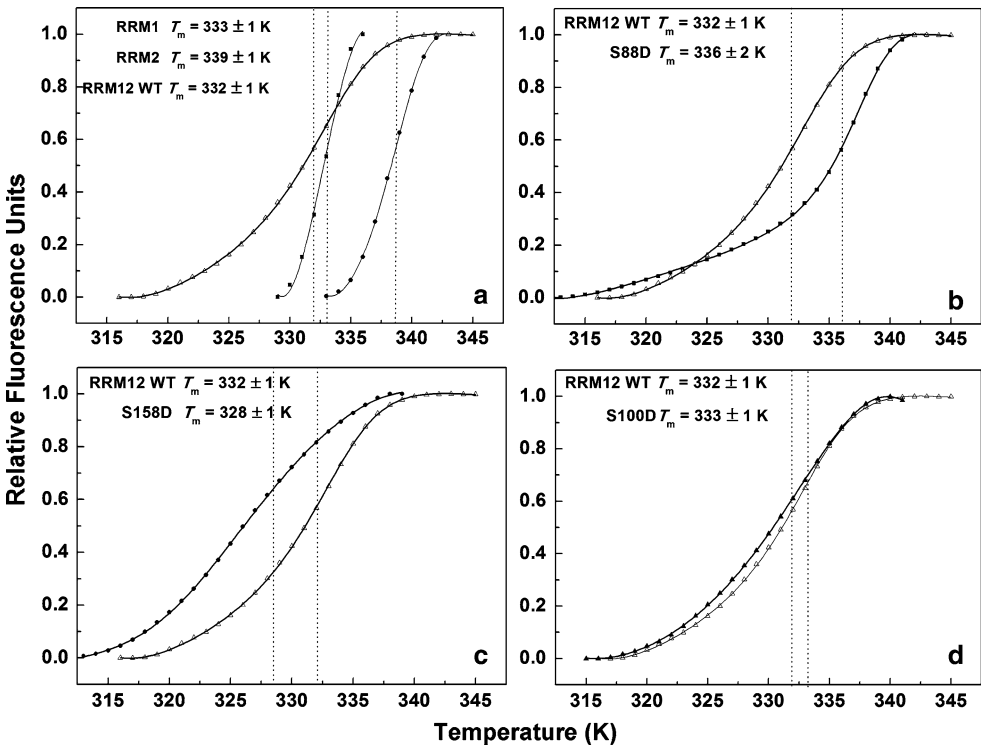

Fig. 5 Effect of phosphomimetic mutations on the thermal stability of HuR. Unfolding thermal denaturation of HuR RRM species and their mutants was determined by DSF by following the fluorescent changes of SYPRO Orange. **a** RRM1 is represented by *filled squares*, RRM2 by *filled circles*, and RRM12 WT by *open triangles*. Ser-by-Asp substitutions are represented as follows: **b** RRM12 S88D (*filled squares*), **c** RRM12 S158D (*filled circles*), and **d** RRM12 S100D (*filled triangles*). Fitted unfolding curves are presented as *solid lines*, superimposed on experimental data. The melting points (T_m) of the transitions are marked by *dashed lines*

Table 3 K_D values of the HuR RRM12 construct and its phosphomimetic mutants, as calculated by CD titration experiments with *c*-fos 11-mer RNA (5′ AUUUUUAUUUU 3′)

Construct	K_D (μM)
RRM12 WT	2.6 ± 0.2
RRM12 S88D	2.7 ± 0.2
RRM12 S100D	2.0 ± 0.1
RRM12 S158D	0.6 ± 0.3

conserved Ser100, which forms part of the short linker between RRM1 and RRM2, displays no significant contributions to the thermal stability of HuR RRM12 upon mutations ($\Delta T_m < 2.0$ K). As expected, the nonphosphorylatable Ser-to-Ala RRM12 mutants behave as RRM12 WT in terms of thermal stability, suggesting that HuR phosphorylation has functional consequences rather than structural effects.

RNA binding of HuR RRM12 is regulated by phosphorylation

To understand how the interaction of HuR-RRM12 with *c*-fos AU-11-mer RNA may be regulated upon phosphorylation, we assessed the affinity of RRM12 WT and its phosphomimetic mutants for the RNA target and explored whether the phosphorylation could modulate recognition in vitro, similarly to in vivo. We used CD to obtain quantitative data over affinities which lie in the μM range. Our CD data show that the affinity of the two RRM1 and RRM2 domains for the RNA is in the low micromolar range (2.6 ± 0.2 μM; Table 3; Fig. 6). Next, we investigated the effect of phosphorylation at RRM1 and at the RRM12 linker by RRM12 S88D and RRM12 S100D mutants, respectively, which show K_D values comparable to that of RRM12 WT (2.7 ± 0.2 μM for S88D and 2.0 ± 0.1 μM for S100D; Table 3). In contrast, RRM12 S158D favors RNA binding (0.6 ± 0.3 μM; Table 3), in agreement what has been previously published in vivo (Doller et al. 2007).

Discussion

HuR consists of three RRM domains, whose function in RNA binding is well characterized, despite the global function and working mechanisms of HuR FL protein not yet being fully understood. The interaction between RRM1 and RRM2 as a tandem construct shows the meaning of the modules and the role of their binding to each other. The combination of the individual RRM domains with additional posttranslational modification sites enables a wide variety of regulation of HuR. With the possibility of being

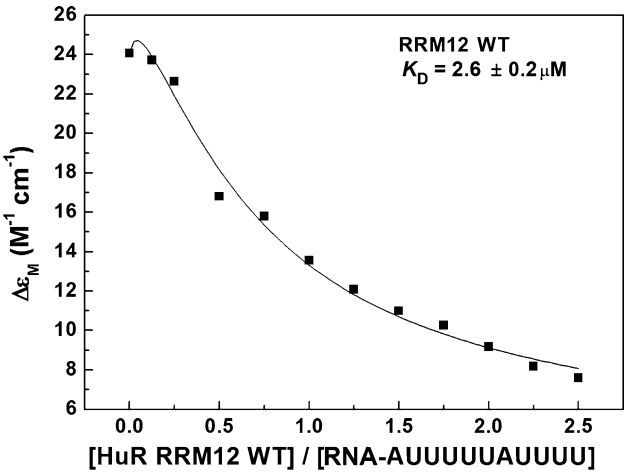

Fig. 6 Changes in the CD signal in the 260–275 nm range of the *c*-fos 11-mer RNA (5′ AUUUUUAUUUU 3′) spectrum during titration with HuR RRM12 WT. Dissociation constant is also shown

phosphorylated (Kim and Gorospe 2008; Kim et al. 2008a, b), methylated (Li et al. 2002), ubiquitinated (Abdelmohsen et al. 2009), submitted to a protease cleavage mechanism (Mazroui et al. 2008), and recently neddylated (Embade et al. 2011), HuR has a huge probability of changing its cellular localization, binding to other proteins, and RNA processing.

Thermal stability studies on HuR species indicate the importance of the cooperation between the two N-terminal RRM domains of HuR, which work as a functional unit. The comparison of T_m values for isolated RRM1 or RRM2 and the two-domain construct RRM12 reveals that RRM12 shows the same thermal stability as RRM1, while RRM2 is substantially more stable. In addition, the fact that the denaturation curve of HuR RRM12 is not the sum of those from the two individual RRM1 and RRM2 domains suggests cooperativity between both modules.

It is tempting to speculate that the RRM12 modular interaction is essential for RNA recognition activity, similarly to what was previously observed for RRM1–RRM2 motifs of the homologous HuD protein upon *c*-fos RNA binding (Wang and Tanaka Hall 2001). Indeed, the preferred orientation between RNA binding domains helps to establish a high-affinity RNA-binding platform (Vitali et al. 2006; Li et al. 2010) and/or to stabilize a suitable conformation that can adapt to the changes in the direction of the RNA chain inside the highly structured 3′ UTRs, as previously suggested (Díaz-Moreno et al. 2010).

To study changes in structure and stability of HuR induced by serine phosphorylation, we designed three Ser-by-Asp mutations. Two of them are localized at the RRM cores, while the third one is in the interdomain linker. No significant changes in secondary structure were observed for none of these phosphomimetic mutants, unlike what has been recently published for other RNA binding domains

(Díaz-Moreno et al. 2009). Therefore, phosphorylation effects on HuR seem to be essentially related to RNA binding properties and/or intermolecular protein interactions rather than to changes of the HuR structure, as confirmed by our CD RNA binding titrations (Fig. 6).

Nevertheless, the thermal stability of HuR constructs is regulated by phosphorylation. The phosphomimetic mutant S88D slightly stabilizes RRM1 in the RRM12 context, which can be explained by the addition of a negative charge to the protein loop mainly governed by two positively charged residues (Benoit et al. 2010). Thus, Asp88 could minimize the electrostatic repulsion between Arg85 and Lys89, which would restrict the loop mobility. In terms of RNA binding, it has been previously reported that in vivo HuR phosphorylation at Ser88 increases the docking of RNA targets to the RNA binding sites (Abdelmohsen et al. 2007b). Also it is proposed that the phosphoserine at position 88 exhibits a Mg^{2+}-ion-mediated interaction with a phosphate group from RNA (Benoit et al. 2010). However, no substantial differences in binding affinities were observed between RRM12 WT and the phosphomimetic RRM12 S88D mutant by performing in vitro CD titrations using *c*-fos RNA.

Slightly destabilizing phosphorylation of Ser158 could be explained based on electrostatic repulsion with another nearby negative residue Glu162, although the negatively charged Asp158 is added at the N-end of helix α_2 of HuR RRM2. Posttranslational modification of Ser158 at RRM2 domain—mimicked by the RRM12 S158D mutation—tightly regulates the binding of HuR RRM12 with *c*-fos RNA in vitro. Actually, the RNA binding affinity of RRM12 S158D is four times larger than that of RRM12 WT, in agreement with previous data in vivo (Doller et al. 2007). Phosphorylation at the level of the RRM12 linker region—Ser100—also has a negligible effect on HuR stability. A plausible explanation is that this solvent-exposed residue does not make many contacts with neighbors. Intriguingly, phosphorylation at Ser100 increases RNA binding in vivo (Abdelmohsen et al. 2007b), although the equivalent serine in the homologous HuD—Ser126—is facing away from the RNA in the HuD/*c*-fos mRNA crystal structure (Wang and Tanaka Hall 2001). In vitro CD titrations reveal no effect of the S100D mutation on RNA recognition with respect to RRM12 WT in vitro. Therefore, phosphorylation at this site would influence RRM2–interdomain linker interactions and the rearrangement between RRM domains, rather than directly repulsing RNA (Benoit et al. 2010).

Perturbations in HuR stability upon posttranslational modifications such as phosphorylation may explain the HuR behavior in binding RNA molecules, as well as in determining their lifetime and translation rate.

Acknowledgments The authors wish to thank Dr. M. Gorospe (NIH, Baltimore, USA) and Dr. J. A. Steitz (Yale University, New Haven, USA) for providing the HuR vectors. We are grateful to Prof. Miguel A. De la Rosa and Dr. Antonio Díaz-Quintana for critical reading of the manuscript. For financial support we thank the Andalusian Government (P07-CVI-02896) and the Spanish Scientific Council Fellowship (JAEpre_08_00375).

References

Abdelmohsen K, Lal A, Kim HH, Gorospe M (2007a) Posttranscriptional orchestration of an anti-apoptotic program by HuR. Cell Cycle 6:1288–1292

Abdelmohsen K, Pullmann R Jr, Lal A, Kim HH, Galban S, Yang X, Blethrow JD, Walker M, Shubert J, Gillespie DA, Furneaux H, Gorospe M (2007b) Phosphorylation of HuR by Chk2 regulates SIRT1 expression. Mol Cell 25:543–557

Abdelmohsen K, Srikantan S, Yang X, Lal A, Kim HH, Kuwano Y, Galban S, Becker KG, Kamara D, de Cabo R, Gorospe M (2009) Ubiquitin-mediated proteolysis of HuR by heat shock. EMBO J 28:1271–1282

Arnold K, Bordoli L, Kopp J, Schwede T (2006) The SWISS-MODEL workspace: a web-based environment for protein structure homology modelling. Bioinformatics 22:195–201

Aroca A, Díaz-Quintana A, Díaz-Moreno I (2011) A structural insight into the C-terminal RNA recognition motifs of T-cell intracellular antigen-1 protein. FEBS Lett 585:2958–2964

Benoit RM, Meisner NC, Kallen J, Graff P, Hemmig R, Cebe R, Ostermeier C, Widmer H, Auer M (2010) The x-ray crystal structure of the first RNA recognition motif and site-directed mutagenesis suggest a possible HuR redox sensing mechanism. J Mol Biol 397:1231–1244

Birney E, Kumar S, Krainer AR (1993) Analysis of the RNA-recognition motif and RS and RGG domains: conservation in metazoan pre-mRNA splicing factors. Nucleic Acids Res 21:5803–5816

Brennan CM, Steitz JA (2001) HuR and mRNA stability. Cell Mol Life Sci 58:266–277

Denkert C, Weichert W, Winzer KJ, Muller BM, Noske A, Niesporek S, Kristiansen G, Guski H, Dietel M, Hauptmann S (2004) Expression of the ELAV-like protein HuR is associated with higher tumor grade and increased cyclooxygenase-2 expression in human breast carcinoma. Clin Cancer Res 10:5580–5586

Díaz-Moreno I, Hollingworth D, Frenkiel TA, Kelly G, Martin S, Howell S, García-Mayoral M, Gherzi R, Briata P, Ramos A (2009) Phosphorylation-mediated unfolding of a KH domain regulates KSRP localization via 14–3-3 binding. Nat Struct Mol Biol 16:238–246

Díaz-Moreno I, Hollingworth D, Kelly G, Martin S, García-Mayoral M, Briata P, Gherzi R, Ramos A (2010) Orientation of the central domains of KSRP and its implications for the interaction with the RNA targets. Nucleic Acids Res 38:5193–5205

Dixon DA, Tolley ND, King PH, Nabors LB, McIntyre TM, Zimmerman GA, Prescott SM (2001) Altered expression of the mRNA stability factor HuR promotes cyclooxygenase-2 expression in colon cancer cells. J Clin Invest 108:1657–1665

Doller A, Huwiler A, Muller R, Radeke HH, Pfeilschifter J, Eberhardt W (2007) Protein kinase C alpha-dependent phosphorylation of the mRNA-stabilizing factor HuR: implications for posttranscriptional regulation of cyclooxygenase-2. Mol Biol Cell 18:2137–2148

Doller A, Pfeilschifter J, Eberhardt W (2008) Signalling pathways regulating nucleo-cytoplasmic shuttling of the mRNA-binding protein HuR. Cell Signal 20:2165–2173

Doller A, Schlepckow K, Schwalbe H, Pfeilschifter J, Eberhardt W (2009) Tandem phosphorylation of serines 221 and 318 by protein kinase Cdelta coordinates mRNA binding and nucleocytoplasmic shuttling of HuR. Mol Cell Biol 30:1397–1410

Embade N, Fernández-Ramos D, Varela-Rey M, Beraza N, Sini M, de Juan VG, Woodhoo A, Martínez-López N, Rodríguez-Iruretagoyena B, Bustamante FJ, de la Hoz AB, Carracedo A, Xirodimas DP, Rodríguez MS, Lu SC, Mato JM, Martínez-Chantar ML (2011) Mdm2 regulates HuR stability in human liver and colon cancer through neddylation. Hepatology. doi:10.1002/hep.24795

Fan XC, Steitz JA (1998) HNS, a nuclear-cytoplasmic shuttling sequence in HuR. Proc Natl Acad Sci U S A 95:15293–15298

Gorospe M (2003) HuR in the mammalian genotoxic response: post-transcriptional multitasking. Cell Cycle 2:412–414

Heinonen M, Bono P, Narko K, Chang SH, Lundin J, Joensuu H, Furneaux H, Hla T, Haglund C, Ristimaki A (2005) Cytoplasmic HuR expression is a prognostic factor in invasive ductal breast carcinoma. Cancer Res 65:2157–2161

Kiefer F, Arnold K, Künzli M, Bordoli L, Schwede T (2009) The SWISS-MODEL repository and associated resources. Nucleic Acids Res 37:D387–D392

Kim HH, Gorospe M (2008) Phosphorylated HuR shuttles in cycles. Cell Cycle 7:3124–3126

Kim HH, Abdelmohsen K, Lal A, Pullmann R Jr, Yang X, Galban S, Srikantan S, Martindale JL, Blethrow J, Shokat KM, Gorospe M (2008a) Nuclear HuR accumulation through phosphorylation by Cdk1. Genes Dev 22:1804–1815

Kim HH, Yang X, Kuwano Y, Gorospe M (2008b) Modification at HuR(S242) alters HuR localization and proliferative influence. Cell Cycle 21:3371–3377

Li H, Park S, Kilburn B, Jelinek MA, Henschen-Edman A, Aswad DW, Stallcup MR, Laird-Offringa IA (2002) Lipopolysaccharide-induced methylation of HuR, an mRNA-stabilizing protein, by CARM1. Coactivator-associated arginine methyltransferase. J Biol Chem 277:44623–44630

Li H, Shi H, Wang H, Zhu Z, Li X, Gao Y, Cui Y, Niu L, Teng M (2010) Crystal structure of the two N-terminal RRM domains of Pub1 and the poly(U)-binding properties of Pub1. J Struct Biol 171:291–297

Ma WJ, Cheng S, Campbell C, Wright A, Furneaux H (1996) Cloning and characterization of HuR, a ubiquitously expressed Elav-like protein. J Biol Chem 271:8144–8151

Mazroui R, Di Marco S, Clair E, von Roretz C, Tenenbaum SA, Keene JD, Saleh M, Gallouzi IE (2008) Caspase-mediated cleavage of HuR in the cytoplasm contributes to pp 32/PHAP-I regulation of apoptosis. J Cell Biol 180:113–127

Meisner NC, Hintersteiner M, Mueller K, Bauer R, Seifert JM, Naegeli HU, Ottl J, Oberer L, Guenat C, Moss S, Harrer N, Woisetschlaeger M, Buehler C, Uhl V, Auer M (2007) Identification and mechanistic characterization of low-molecular-weight inhibitors for HuR. Nat Chem Biol 3:508–515

Niesen FH, Berglund H, Vedadi M (2007) The use of Differential Scanning Fluorimetry to detect ligand interactions that promote protein stability. Nat Protoc 2:2212–2221

Pettersen EF, Goddard TD, Huang CC, Couch GS, Greenblatt DM, Meng EC, Ferrin TE (2004) UCSF Chimera—a visualization system for exploratory research and analysis. J Comput Chem 25:1605–1612

Privalov PL (1979) Stability of proteins: small globular proteins. Adv Protein Chem 33:167–241

Santoro MM, Bolen DW (1988) Unfolding free energy changes determined by the linear extrapolation method. 1. Unfolding of phenylmethane sulfonyl alpha-chymotrypsin using different denaturants. Biochemistry 27:8063–8068

Sengupta S, Jang BC, Wu MT, Paik JH, Furneaux H, Hla T (2003) The RNA-binding protein HuR regulates the expression of cyclooxygenase-2. J Biol Chem 278:25227–25233

Sreerama N, Woody RW (2000) Estimation of protein secondary structure from Circular Dichroism spectra: comparison of CONTIN, SELCON, and CDSSTR methods with an expanded reference set. Anal Biochem 287:252–260

Vitali F, Henning A, Oberstrass FC, Hargous Y, Auweter SD, Erat M, Allain FH (2006) Structure of the two most C-terminal RNA recognition motifs of PTB using segmental isotope labeling. EMBO J 25:150–162

Wang X, Tanaka Hall TM (2001) Structural basis for recognition of AU-rich element RNA by the HuD protein. Nat Struct Biol 8:141–145